

Direct Simulation Monte Carlo for Atmospheric Entry

1. Theoretical Basis and Physical Models

Iain D. Boyd

Department of Aerospace Engineering
University of Michigan
Ann Arbor, Michigan, USA

iainboyd@umich.edu

ABSTRACT

The direct simulation Monte Carlo method (DSMC) has evolved over 40 years into a powerful numerical technique for the computation of complex, nonequilibrium gas flows. In this context, nonequilibrium means that the velocity distribution function is not in an equilibrium form due to a low number of intermolecular collisions within a fluid element. In atmospheric entry, nonequilibrium conditions occur at high altitude and in regions of flow fields with small length scales. In this first article of two parts, the theoretical basis of the DSMC technique is discussed. In addition, the methods used in DSMC are described for simulation of high temperature, real gas effects and gas-surface interactions. The current status of the various models is reviewed and areas where further work is required are identified.

1.0 INTRODUCTION

The analysis of dilute gas flows at all Knudsen numbers can be derived from the Boltzmann equation that describes the evolution of the molecular velocity distribution function (VDF) [1]. In the absence of a body force, the Boltzmann equation is written:

$$\frac{\partial}{\partial t}(nf) + \bar{C} \cdot \frac{\partial}{\partial \bar{r}}(nf) = \Delta(f) \quad (1.1)$$

where f is the VDF, n is the number density, \bar{C} is the particle velocity vector, \bar{r} is the particle position vector, t is time, and $\Delta(f)$ represents the rate of change in the VDF due to collision processes. The equilibrium solution of the Boltzmann equation is the Maxwellian VDF:

$$f(\bar{C})d\bar{C} = \left(\frac{m}{2\pi kT}\right)^{3/2} \exp\left(-\frac{mC^2}{2kT}\right)d\bar{C} \quad (1.2)$$

where m is the mass of a particle, k is Boltzmann's constant, and T is the temperature. The physical mechanism that maintains the VDF in equilibrium is inter-molecular collisions, and so a gas falls into a nonequilibrium state under conditions where there is not a large enough number of collisions occurring to maintain equilibrium. The two main physical flow conditions that lead to nonequilibrium are low density and

Report Documentation Page

Form Approved
OMB No. 0704-0188

Public reporting burden for the collection of information is estimated to average 1 hour per response, including the time for reviewing instructions, searching existing data sources, gathering and maintaining the data needed, and completing and reviewing the collection of information. Send comments regarding this burden estimate or any other aspect of this collection of information, including suggestions for reducing this burden, to Washington Headquarters Services, Directorate for Information Operations and Reports, 1215 Jefferson Davis Highway, Suite 1204, Arlington VA 22202-4302. Respondents should be aware that notwithstanding any other provision of law, no person shall be subject to a penalty for failing to comply with a collection of information if it does not display a currently valid OMB control number.

1. REPORT DATE SEP 2009	2. REPORT TYPE N/A	3. DATES COVERED -	
4. TITLE AND SUBTITLE Direct Simulation Monte Carlo for Atmospheric Entry 1. Theoretical Basis and Physical Models		5a. CONTRACT NUMBER	
		5b. GRANT NUMBER	
		5c. PROGRAM ELEMENT NUMBER	
6. AUTHOR(S)		5d. PROJECT NUMBER	
		5e. TASK NUMBER	
		5f. WORK UNIT NUMBER	
7. PERFORMING ORGANIZATION NAME(S) AND ADDRESS(ES) Department of Aerospace Engineering University of Michigan Ann Arbor, Michigan, USA		8. PERFORMING ORGANIZATION REPORT NUMBER	
9. SPONSORING/MONITORING AGENCY NAME(S) AND ADDRESS(ES)		10. SPONSOR/MONITOR'S ACRONYM(S)	
		11. SPONSOR/MONITOR'S REPORT NUMBER(S)	
12. DISTRIBUTION/AVAILABILITY STATEMENT Approved for public release, distribution unlimited			
13. SUPPLEMENTARY NOTES See also ADA562449. RTO-EN-AVT-162, Non-Equilibrium Gas Dynamics - From Physical Models to Hypersonic Flights (Dynamique des gaz non- equilibres - Des modeles physiques jusqu'au vol hypersonique)., The original document contains color images.			
14. ABSTRACT The direct simulation Monte Carlo method (DSMC) has evolved over 40 years into a powerful numerical technique for the computation of complex, nonequilibrium gas flows. In this context, nonequilibrium means that the velocity distribution function is not in an equilibrium form due to a low number of intermolecular collisions within a fluid element. In atmospheric entry, nonequilibrium conditions occur at high altitude and in regions of flow fields with small length scales. In this first article of two parts, the theoretical basis of the DSMC technique is discussed. In addition, the methods used in DSMC are described for simulation of high temperature, real gas effects and gas-surface interactions. The current status of the various models is reviewed and areas where further work is required are identified.			
15. SUBJECT TERMS			
16. SECURITY CLASSIFICATION OF:			17. LIMITATION OF ABSTRACT
a. REPORT unclassified	b. ABSTRACT unclassified	c. THIS PAGE unclassified	SAR
			18. NUMBER OF PAGES 28
			19a. NAME OF RESPONSIBLE PERSON

small length scales. A low density leads to a reduced collision rate while a small length scale reduces the size of a fluid element. The usual metric for determining whether a particular gas flow is in a state of nonequilibrium is the Knudsen number defined as follows:

$$Kn = \frac{\lambda}{L} \quad (1.3)$$

where λ is the mean free path of the gas and L is the characteristic length scale. The mean free path is the average distance traveled by each particle between collisions and is given for a hard sphere by

$$\lambda = \frac{1}{\sqrt{2}n\sigma} \quad (1.4)$$

where n is again the number density, and σ is the hard sphere collision cross section. Thus, at low density, the mean free path (and therefore Kn) becomes large. Similarly, for small length scales, L becomes small and again Kn becomes large. As a guiding rule, it is generally accepted that kinetic nonequilibrium effects become important when $Kn > 0.01$.

At a Knudsen number near zero, the velocity distribution function everywhere in a flow field has the Maxwellian form, there are no molecular transport processes, such as viscosity and thermal conductivity, and the flow may be modeled using the Euler equations. Indeed, the Euler equations of fluid flow can be derived by taking moments of the Boltzmann equation and evaluating them using the Maxwellian VDF. As the Knudsen number increases up to values below 0.01, the velocity distribution function in the flow field may be represented as a small perturbation from the equilibrium Maxwellian form that is known as the Chapman-Enskog distribution [1]. Evaluation of moments of the Boltzmann equation using the Chapman-Enskog VDF leads to the Navier-Stokes equations in which shear stress and heat flux depend linearly on the spatial gradients of velocity and temperature, respectively. As the Knudsen number rises above 0.01, these linear transport relations are unable to accurately describe the strong nonequilibrium processes. It is then necessary to develop higher order sets of partial differential equations (such as the Burnett equations) or to solve the Boltzmann equation. While there has been some success achieved in formulating and solving the Burnett equations, there remain issues with boundary conditions, and it is not clear that the amount of additional Knudsen number range provided is worth the significant additional effort in numerical analysis. Unfortunately, development of robust and general numerical solution schemes for the Boltzmann equation has also proved a significant challenge. Again, some progress has been made, but there is still much work to be done to be able to simulate all of the flow physics of interest in real world problems.

The direct simulation Monte Carlo (DSMC) method was first introduced by Graeme Bird in 1961 [2] specifically to analyze high Knudsen number flows. Since that time, Bird has written two books on the method [3,4] and thousands of research papers have been published that report on development and application of the technique. The significance of the DSMC technique has been its ability over 40 years of development to fill the void described above in gas analysis methodology for high Knudsen number flows. The DSMC technique emulates the same physics as the Boltzmann equation without providing a direct solution. The DSMC method follows a representative set of particles as they collide and move in physical space. It has been demonstrated that DSMC converges to solution of the Boltzmann equation in the limit of a very large number of particles [4].

High Knudsen number conditions arise in many areas of science and technology including space and atmospheric science, vapor processing of materials, spacecraft propulsion systems, and micro-scale gas flows. Atmospheric entry flow conditions may fall into the kinetic nonequilibrium regime at sufficiently low density

(that occurs at high altitude in a planet's atmosphere) and for very small entry shapes (e.g. meteoroids that have a diameter on the order of a centimeter [5]). In addition, situations arise where localized regions of a flow may contain low density (e.g. the wake behind a capsule) or small length scales (e.g. sharp leading edges on a vehicle, or shock waves and boundary layers that may have very steep spatial gradients in flow field properties).

For hypersonic flows, it is a valid question to ask whether high Knudsen number phenomena lead to effects that are of practical significance. Recent detailed studies [6,7] have compared DSMC and CFD computations of hypersonic flows over cylinders and wedges for global Knudsen numbers ranging from continuum ($Kn=0.002$) to rarefied ($Kn=0.25$). The focus of the studies was the effect of any nonequilibrium flow phenomena on surface properties such as drag and heat transfer. It was found at $Kn=0.002$ that DSMC and CFD gave identical results for all surface properties including drag force and peak heat transfer. However, as Kn was increased, the differences between DSMC and CFD surface results also grew larger. For example, in Mach 25 flow of nitrogen over a cylinder at the highest Knudsen number of 0.25, in comparison to CFD, DSMC predicted a 23% lower drag force and a 29% lower peak heat flux. These differences are clearly significant and indicate that accurate determination of surface properties in high Knudsen number flows does require a non-continuum, kinetic approach, such as DSMC.

An important part of the success of the DSMC technique in analyzing high Knudsen number atmospheric entry flows, has been the ability to include in the technique models that are effective in simulating high temperature, real gas effects. Such effects include mixtures of chemical species, relaxation of internal energy modes, chemical reactions such as dissociation and ionization, radiation, and gas-surface interaction. In this article, the fundamental aspects of the DSMC technique are described with an emphasis on physical modeling issues related to its application to hypersonic, atmospheric entry problems and the simulation of the associated real gas effects. Examples are provided that illustrate the current capabilities of these models and areas where further work is needed are identified. The second part of this article [8] reviews the current status of existing DSMC codes and their application to analysis of hypersonic entry flows.

2.0 BASIC ALGORITHM OF THE DSMC TECHNIQUE

The DSMC technique emulates the physics of the Boltzmann equation by following the motions and collisions of a large number of model particles. Each particle possesses molecular level information including a position vector, a velocity vector, and physical information such as mass and size. Particle motion and collisions are decoupled over a time step Δt that is smaller than the local mean free time. During the movement of particles, boundary conditions such as reflection from solid surfaces are applied. The physical domain to be simulated in a DSMC computation is covered by a mesh of cells. These cells are used to collect together particles that may collide. There are a number of DSMC schemes for simulating collisions and all of them achieve a faster numerical performance than the molecular dynamics (MD) method [9] by ignoring the influence of the relative positions of particles within a cell in determining particles that collide. This simplification requires that the size of each cell be less than the local mean free path of the flow. Bird's No Time Counter (NTC) scheme [4] is the most widely used collision scheme in which a number of particle pairs in a cell are formed that is given by:

$$N_c = \frac{1}{2} n \bar{N} (\sigma g)_{\max} \Delta t \quad (2.1)$$

where n is the number density, \bar{N} is the average number of particles in the cell, σ is the collision cross section, and g is the relative velocity. Each of the N_c pairs of particles is formed at random regardless of position in the cell, and then a probability of collision for each pair is evaluated using:

$$P_c = \frac{\sigma g}{(\sigma g)_{\max}} \quad (2.2)$$

This procedure reproduces the expected equilibrium collision rate under conditions of equilibrium. It is determined whether the particle pair actually collides by comparing the collision probability, P_c , to a random number. When a collision occurs, post-collision velocities are calculated using conservation of momentum and energy.

The cells employed for simulating collisions are also often used for the sampling of macroscopic flow properties such as density, velocity, and temperature. There is no necessity to have the collision and sampling cells be identical, however, and sometimes a coarser mesh is used for sampling.

The basic steps in each iteration of the DSMC method are: (1) move particles over the time step Δt ; (2) apply boundary conditions such as introducing new particles at inflow boundaries, removing particles at outflow boundaries, and processing reflections at solid boundaries; (3) sort particles into cells and calculate collisions; and (4) sample average particle information. As an example of how sampled particle information is employed to determine a macroscopic flow property, the average mass density in a computational cell of volume V is given by

$$\rho = \frac{\sum_{i=1}^{N_p} m_i}{V \times N_t} \quad (2.3)$$

where m_i is the mass of particle i , N_p is the total number of particles that have occupied this cell over N_t iterations of the computation. Also, as an illustration of the determination of surface properties, for a surface element of area A , the average shear stress is given by

$$\tau_w = \frac{\sum_j m_j (u_j^i - u_j^r)}{A \times N_t \times \Delta t} \quad (2.4)$$

where u_j^i and u_j^r are the incident and reflected velocity components tangent to the surface element of each particle j to hit the element during N_t iterations of the computation.

A simulation begins from some initial condition, and a finite number of iterations must elapse in order for the flow to reach a steady state. Generally, steady state is detected as a leveling off of the total number of particles in the simulation. After steady state is reached, sampling of flow field and surface properties begins and the simulation is continued a further number of iterations in order to reduce the statistical noise in the sampled information to an acceptable level. A typical DSMC computation may employ one million particles, reach steady state after 50,000 iterations, and continue sampling for a further 50,000 iterations. On a modern desktop computer, such a simulation should take about 3 hours.

While the ideas behind the DSMC technique are simple, implementation in an algorithm takes on many different forms. Specific DSMC algorithms have been developed for vector computers [10] and parallel computers [11,12]. Bird has focused work on customizing the algorithm to achieve efficient performance on single processor machines [13]. Some of the most commonly used DSMC codes are summarized in the second part of this article [8] in which examples of their application to various atmospheric entry flows are also discussed.

Having provided a general overview of the basic elements of the DSMC method, in the following sections some of the physical models are described that are most critical to the application of the DSMC technique to analyze hypersonic entry flows.

3.0 PHYSICAL MODELS OF THE DSMC TECHNIQUE

In this section, the most commonly employed physical models are reviewed for DSMC computation of hypersonic entry flows. The basic ideas are described for simulation of a number of physical phenomena including momentum exchange, internal energy relaxation, chemical reactions, and gas-surface interactions. Where possible, examples are provided of attempts to validate these models using laboratory data.

3.1 Elastic Momentum Exchange

In the absence of internal energy exchange and chemical reactions, an elastic collision between two particles leads only to changes in their velocity (or momentum) components. The frequency of such interactions is determined by the collision cross section and a number of such models have been developed for DSMC. The most widely used forms are the Variable Hard Sphere (VHS) [14] and the Variable Soft Sphere (VSS) [15]. For hypersonic flow, the VHS model is considered sufficiently accurate, for which the cross section is given as:

$$\sigma = \sigma_{ref} \left(\frac{g}{g_{ref}} \right)^{-2\omega} \quad (3.1)$$

where σ_{ref} and g_{ref} are reference values, and ω is related to the viscosity temperature exponent. Specifically, it is assumed that the gas viscosity is described by a simple temperature relation:

$$\mu = \mu_{ref} \left(\frac{T}{T_{ref}} \right)^{0.5+\omega} \quad (3.2)$$

and the relationship between the reference parameters is provided by Bird [4]. Values of these reference parameters for many common species are provided in Bird [4] and these are generally obtained by comparison with measured or computed viscosity data. For the VHS model, isotropic scattering is assumed in which the unit vector of the post-collision relative velocity is assigned at random on the unit sphere. The VSS model represents an improvement over VHS in that it allows collision parameters to be determined through comparison with both viscosity and diffusivity data. The VSS cross section is the same as the VHS model, but the scattering angle is given by:

$$\chi = 2 \cos^{-1} \left\{ \left(\frac{b}{d} \right)^{1/\alpha} \right\} \quad (3.3)$$

where α is determined from diffusivity data, b is the distance of closest approach and d is the collision diameter. Again, values of α for common gases are provided by Bird [4]. Note that $\alpha=1$ corresponds to the VHS model.

One of the most common test cases for evaluation of the DSMC technique in simulating nonequilibrium flows involving only elastic momentum exchange are normal shock waves of noble gases. Figure 1a shows the density profile through a normal shock wave at Mach 9 for argon. Detailed measurements were obtained using an electron beam technique by Alsmeyer at a number of different Mach numbers in both argon and nitrogen [16]. Included in Fig. 1a are both DSMC and CFD results. The DSMC computations used the VHS model while the CFD results solved the Navier-Stokes equations with the viscosity given by the same VHS parameters used in DSMC. The comparison shows that the DSMC technique is able to reproduce the measured data very accurately whereas CFD predicts a shock wave that is too thin. Figure 1b shows the reciprocal shock thickness (a measure of the density gradient at $x / \lambda = 0$) for all the argon shock waves investigated by Alsmeyer [16]. Once again, it is clear that DSMC provides excellent agreement with the measurements for all conditions considered. CFD consistently predicts an inverse shock thickness that is too large (that is, shocks that are too thin) for all Mach numbers above about 1.50. Another compelling validation of the capability of DSMC in simulating nonequilibrium hypersonic flows is provided by the comparisons shown in Figs. 2a and 2b. These plots are taken from the study by Pham-Van-Diep et al. [17] in which velocity distribution functions were examined inside a normal shock of helium at Mach 25. Figure 2a shows the distributions in the front of the shock for the parallel (circles and solid line) and perpendicular (triangles and dashed line) velocity components. Symbols represent electron beam measurements and lines represent DSMC computations that employed a detailed Maitland-Smith collision model. The horizontal axis in these plots is reversed so that the high freestream parallel velocity component appears as a peak towards the left of the figure. The parallel velocity distribution shows a strong nonequilibrium profile with the higher velocity, lower temperature peak on the left, and a higher temperature, lower velocity peak towards the middle. The distribution of the perpendicular component is centered on zero and also consists of two distinct populations from the low temperature freestream and the high temperature post-shock regions. The profiles in Fig. 2b are obtained further downstream towards the middle of the shock and continue to show strongly nonequilibrium behavior. Clearly, the Navier-Stokes equations, that are based on a small perturbation from equilibrium, are not able to accurately model such phenomena. The excellent agreement with measured data shown in these plots is one of the strongest illustrations of the ability of the DSMC technique to reproduce nonequilibrium flow at the level of the distribution functions.

The main limitation of the VHS/VSS collision models is their reliance on the ability to model viscosity and diffusivity as a simple function of temperature. Even for the common gases for which VHS/VSS parameters are provided by Bird [4], the viscosity dependence on temperature may change over a sufficiently wide temperature range. For illustration of the types of problems encountered with the VHS/VSS models, Figs. 3a and 3b show collision cross sections as a function of collision energy for two different collisions involving electrons. For such interactions, direct measurements of cross sections are available in the literature. Various attempts to fit the measured data using the VHS model are shown that demonstrate limitations of the VHS model for describing these interactions. Indeed, a negative value of ω must be employed in VHS in order to approach the measured trends. More details of these cross section evaluations are provided in [18].

3.2 Rotational Energy Exchange

The DSMC technique usually simulates the internal energy modes of atoms and molecules by assigning rotational, vibrational, and electronic energies to each particle. In hypersonic flows, generally the electronic modes are ignored, as is the case for CFD studies. Analysis of jet flows including electronic energy is described for example in [19]. We focus here on rotational and vibrational energy exchange.

The rotational mode is usually simulated using a classical physics approach in which the rotational energy, ε_r , is assumed continuously distributed at equilibrium according to a Boltzmann distribution:

$$f(\varepsilon_r)d\varepsilon_r = \frac{1}{\Gamma(\zeta/2)} \left(\frac{\varepsilon_r}{kT}\right)^{\zeta/2-1} \exp\left(-\frac{\varepsilon_r}{kT}\right) d\left(\frac{\varepsilon_r}{kT}\right) \quad (3.4)$$

where ζ is the number of rotational degrees of freedom (=2 for a diatomic molecule; =3 for a polyatomic molecule), k is Boltzmann's constant, and T is the temperature.

When a particle representing a molecule is injected into a DSMC computation, it is given an initial rotational energy sampled from Eq. (3.4). The rotational energy of the particle can change through collisions with other particles and through collisions with a solid surface (see section 3.7). In a continuum analysis of rotational energy exchange, the rotational relaxation equation is usually employed:

$$\frac{de_r}{dt} = \frac{e_r^* - e_r}{\tau_r} \quad (3.5)$$

where e_r is the specific rotational energy, e_r^* is the equilibrium value at temperature T , and τ_r is the rotational relaxation time. The equivalent DSMC procedure involves evaluating a probability of rotational energy exchange for each collision followed by appropriate energy exchange mechanics for those collisions that lead to rotational relaxation. The average probability of rotational energy exchange is:

$$\langle P_{rot} \rangle = \frac{1}{Z_{rot}} = \frac{\tau_t}{\tau_r} = \frac{1}{\tau_r \nu} \quad (3.6)$$

where Z_{rot} is the rotational collision number, τ_t is the translational relaxation time that is equal to the inverse of the collision frequency, ν . Boyd [20] developed the following instantaneous rotational energy exchange probability based on Parker's model [21] for the rotational collision number and the VHS collision model:

$$P_{rot} = \frac{1}{(Z_{rot})_\infty} \left(1 + \frac{\Gamma(\zeta + 2 - \omega)}{\Gamma(\zeta + 3/2 - \omega)} \left(\frac{kT^*}{\varepsilon_{tot}}\right)^{\frac{1}{2}} \frac{\pi^{\frac{3}{2}}}{2} + \frac{\Gamma(\zeta + 2 - \omega)}{\Gamma(\zeta + 1 - \omega)} \left(\frac{kT^*}{\varepsilon_{tot}}\right) \left(\frac{\pi^2}{4} + \pi\right) \right) \quad (3.7)$$

where ε_{tot} is the total collision energy (the sum of the translational collision energy and the rotational energy), T^* is the characteristic temperature of the intermolecular potential, and $(Z_{rot})_\infty$ is the limiting value. After evaluation of the rotational energy exchange probability, a random number is used to decide whether the collision leads to energy exchange. For those collisions involving rotational energy exchange, the Borgnakke-Larsen (BL) model [22] is employed to assign new post-collision rotational energies. The BL model assumes local thermodynamic equilibrium to sample the fraction of the total collision energy due to rotation, $\varepsilon_{rot}/\varepsilon_{tot}$, from the following expression:

$$\frac{P}{P_{\max}} = \left(\frac{\zeta + 1 - \omega}{2 - \omega} \left(1 - \frac{\varepsilon_{rot}}{\varepsilon_{tot}} \right) \right)^{2-\omega} \left(\frac{\zeta + 1 - \omega}{\zeta - 1} \left(\frac{\varepsilon_{rot}}{\varepsilon_{tot}} \right) \right)^{\zeta-1} \quad (3.8)$$

Once the new rotational energy is assigned, the remaining energy is the new translational energy and hence determines the new post-collision relative velocity. The regular DSMC collision mechanics is then performed to calculate the velocities of the colliding particles.

Lumpkin et al. [23] noted that an additional correction must be applied to any DSMC rotational energy exchange probability in order to make Borgnakke-Larsen exchange mechanics consistent with the continuum rotational relaxation equation, Eq. (3.5). The form of the correction is:

$$P_{particle} = P_{continuum} \left(1 + \frac{2\zeta}{4 - 2\omega} \right) \quad (3.9)$$

that is usually close to a factor of two.

While the rotational energy is usually simulated in the classical limit, a quantum mechanical approach has also been developed by Boyd [24].

A detailed set of experimental measurements of hypersonic normal shock waves in nitrogen was collected by Robben and Talbot [25]. Again, an optical diagnostic technique was employed to measure both the density and the rotational energy distribution function through the shock wave for a number of different Mach numbers. Figure 4a compares DSMC simulations [24] with the measurements of the density and rotational temperature profiles at a Mach number of 12.9. Clearly, very good agreement between simulation and measurement is obtained. Figure 4b shows rotational energy distribution functions measured at four different locations in this same shock wave, moving from upstream to downstream through (a) to (d). Once again, the excellent agreement obtained between DSMC and experiment at the level of the distribution function is one of the strongest illustrations of the ability of the technique to accurately simulate nonequilibrium phenomena. The main limitation of the Robben and Talbot data is that it was collected for a flow with a total temperature of just 300 K. There is a strong requirement for additional, detailed measured data sets for true hypersonic, entry conditions.

3.3 Vibrational Energy Exchange

The simulation of vibrational relaxation follows a similar procedure to that for rotation. The average probability of vibrational energy exchange is typically evaluated using the vibrational relaxation time used in hypersonic CFD models due to Millikan and White [26] with the Park high temperature correction [27]:

$$\tau_{vib} = \tau_{MW} + \tau_{Park} \quad (3.10)$$

In order to accurately reproduce this vibrational relaxation time in a DSMC computation, due to its complex temperature dependence, it is necessary to evaluate a collision averaged vibrational exchange probability [28]. Unlike rotational relaxation, a quantum mechanical approach is almost always employed for simulation of vibrational energy relaxation in hypersonic flows. A quantized vibrational energy exchange model corresponding to the classical Borgnakke-Larsen approach was formulated by Bergemann and Boyd [29]. It involves first determining the maximum vibrational quantum level available based on the total collision energy:

$$v_{\max} = \left\lfloor \frac{\varepsilon_{tot}}{k\theta_v} \right\rfloor \quad (3.11)$$

where ε_{tot} is the total collision energy (the sum of the translational collision energy and the vibrational energy), $\lfloor \rfloor$ means truncation, and θ_v is the characteristic temperature for vibration of the molecule. Then, the post-collision vibrational quantum number, v , is sampled from:

$$\frac{P}{P_{\max}} = \left(1 - \frac{vk\theta_v}{\varepsilon_{tot}} \right)^{1-\omega} \quad (3.12)$$

The Lumpkin et al. [23] correction factor must also be applied to the vibrational exchange probability.

More detailed vibrational relaxation models for DSMC have also been developed and applied to hypersonic flows. For example, in [30], the Multiple Quantum-Step Transition (MQST) model was developed for use in DSMC. Based on the Forced Harmonic Oscillator (FHO) model of Kerner [31], the probability of a multi-quantum activation is given by:

$$P_{v,v+\Delta v} = v!(v+\Delta v)! \exp(-\varepsilon_1) \varepsilon_1^{2v+\Delta v} \left| \sum_{k=0}^v \frac{(-1)^k \varepsilon_1^{-k}}{k!(v-k)!(v+\Delta v-k)!} \right|^2 \quad (3.13)$$

with

$$\varepsilon_1 = a \exp(-g^*/g) \quad (3.14)$$

where constants a and g^* are determined from molecular parameters. The corresponding deactivation probability is developed in [30] based on detailed balance. The MQST model was compared in [30] to the Borgnakke-Larsen (B-L) approach for flow of nitrogen at a velocity of 5.1 km/s over a 10 cm radius sphere at 80 km altitude. Figure 5 compares the computed vibrational energy distribution functions at the point of maximum vibrational temperature in the shock layer. The Boltzmann distribution corresponds to the maximum vibrational temperature. Clearly, both the phenomenological B-L model and the more detailed MQST model predict a significant degree of vibrational nonequilibrium. It is interesting to note that the B-L model predicts a higher level of nonequilibrium.

There are no measurements in the literature of vibrational energy distribution functions in hypersonic flows that can be used to validate the DSMC vibrational relaxation models. One of the most useful sets of data was obtained by Sharma [32] in a shock-tube for flow of N_2 at a velocity of 6.2 km/s. Using spectroscopy, both the rotational and vibrational temperatures of N_2 were inferred at two different points in the shock wave as shown in Fig. 6. The DSMC computations [28] shown in Fig. 6 employed the B-L approach and show reasonable agreement with the measured data. Further more detailed experiments of this kind are required to more completely validate the DSMC simulation approach for vibrational relaxation.

3.4 Chemical Reactions

The most commonly used DSMC chemistry model is the Total Collision Energy (TCE) model of Bird [4]. This model is based on a modified Arrhenius rate coefficient of the form:

$$C = aT^b \exp\left(-\frac{\varepsilon_{act}}{kT}\right) \quad (3.15)$$

where a and b are constants, and ε_{act} is the activation energy of the reaction. By integrating over the equilibrium distribution function for the total collision energy, it may be shown that the form of the reaction probability consistent with Eq. (3.15) for the VHS collision model is given by:

$$P_{TCE} = A \frac{(\varepsilon_{tot} - \varepsilon_{act})^{b+\zeta+\frac{1}{2}}}{(\varepsilon_{tot})^{\zeta+1-\omega}} \quad (3.16)$$

where ε_{tot} is the total collision energy of all modes of both particles participating in the collision, and constant A depends on the Arrhenius parameters and molecular constants. The TCE model was extended to include the important physical phenomenon of vibration-dissociation coupling by Haas and Boyd [33] in the Vibrationally Favored Dissociation (VFD) model. The VFD model makes it possible to increase the dissociation probability of particles having large vibrational energy:

$$P_{VFD} = A \frac{(\varepsilon_{tot} - \varepsilon_{act})^{b+\zeta+\frac{1}{2}}}{(\varepsilon_{tot})^{\zeta+1-\omega}} (\varepsilon_{vib})^\phi \quad (3.17)$$

Values of the VFD parameters for air molecules have been determined through comparison with experimental data. For example, Fig. 7 shows comparisons [33] for dissociation incubation distances between DSMC predictions and data measured by Hornung [34] in hypersonic flows of N_2 .

Measurements of reaction cross sections of interest in hypersonic air flows are not generally available, except for some reactions involving electrons. As *ab initio* computational chemistry techniques mature, there is the hope in the future that detailed computed data bases can be used to help develop more accurate DSMC chemistry models. One example of such a database was constructed using a Quasi-Classical Trajectory (QCT) method by Bose and Candler [35] for the Zeldovich exchange reaction:



This QCT database was employed [36] to perform a detailed evaluation of the TCE model for this particular reaction. Figure 8a shows reaction cross sections as a function of translational collision energy, at a particular rotational energy level ($J=64$) of the reactant, N_2 , for three different reactant vibrational levels ($v=0, 7, 13$). Clearly, the TCE model is not at all accurate for this reaction in terms of collision cross section. This poor comparison motivated the development of another DSMC chemistry model that allows favoring from each of the translational, rotational and vibrational energy modes. Termed the Generalized Collision Energy (GCE) model, the reaction probability is given by [36]:

$$P_{GCE} = A \frac{(\varepsilon_{tot} - \varepsilon_{act})^{b+\zeta+\frac{1}{2}}}{(\varepsilon_{tot})^{\zeta+1-\omega}} (\varepsilon_{vib})^\phi (\varepsilon_{tra})^\alpha (1 - \varepsilon_{rot}/\varepsilon_{tot})^\beta \quad (3.19)$$

Figure 8b provides comparisons between the QCT data and the GCE reaction cross sections. While the comparisons are far from perfect, they represent a significant improvement over the TCE model. For this particular reaction, the GCE model parameter values were: $\alpha=0.2$, $\beta=-0.5$, $\phi=0.3$.

The detailed QCT database makes it possible to evaluate several aspects of DSMC chemistry modeling. The second aspect concerns the energy distribution of the particles selected for reaction. Figure 9a shows the vibrational energy distribution function of the reacting N_2 molecules under a thermal equilibrium condition where all mode temperatures are at 5,000 K. Clearly, the GCE model provides almost perfect agreement with the QCT data. A similar level of agreement is shown in Fig. 9b for a strongly nonequilibrium condition similar to that expected in hypersonic entry flow at high altitude.

When it is determined in a DSMC computation that a chemical reaction occurs, the activation energy is removed from the total collision energy, then Borgnakke-Larsen procedures are used to distribute the remaining energy among the energy modes of the product particles. Once again, the QCT database allows this aspect of DSMC chemistry modeling to be assessed. Figures 10a and 10b show the vibrational energy distributions of the product NO molecules for the same two conditions shown in Figs. 9a and 9b. Once again, the GCE model provides remarkably accurate simulation of the detailed phenomena captured by the QCT analysis. It is planned in the near future to conduct further comparisons of this nature for important hypersonic flow reactions such as dissociation and ionization.

Recently, details of simulating backward chemical rate processes with the DSMC technique have been discussed by Boyd [37]. An important issue here is that the TCE model, and its derivatives like VFD and GCE, all depend on the use of a rate coefficient expressed in Arrhenius form. Backward rate coefficients are generally evaluated as the quotient of the forward rate coefficient and the equilibrium constant that is usually a highly complex function of temperature. Thus, it is not generally possible to express the backward rate coefficient in the simple Arrhenius form. This problem is either addressed by performing a best-fit of the true backward rate coefficient to an Arrhenius form over a temperature range of interest, or by calculating the temperature in each cell of the DSMC computation in order to evaluate the equilibrium constant exactly [37].

While the DSMC method is based on the premise of a dilute gas for which three body collisions are ignored, it is sometimes important to include recombination in DSMC calculations and models for such reactions are presented in [4] and [28].

Several other DSMC chemistry models relevant to hypersonic entry flows have been developed including the maximum entropy model [38], the weak vibrational bias model [39], the threshold line model [40], and the model of Rebick and Levine [41]. Many of the models are reviewed and evaluated in [42] and [43].

3.5 Charged Species

Ions and electrons are formed in sufficiently energetic hypersonic flows first through associative ionization and then through electron impact ionization. While these reactions can be simulated using the TCE chemistry model with DSMC, the presence of electrons in a DSMC computation presents some special challenges. Specifically, due to their very low mass relative to other species: (1) the thermal velocity of an electron is orders of magnitude higher than for other species; and so (2) the collision frequency of electrons is orders of magnitude higher than for other species. If an electron was not charged, then the first problem would simply require use of a much smaller time step Δt than would be required otherwise. However, electrostatic attraction means that electrons and ions interact with one another such that electron diffusion is reduced and ion diffusion is slightly increased. A common model to describe this behavior is ambi-polar diffusion in which it is assumed that ions and electrons diffuse at the same rate. Bird [44] first introduced a DSMC model for ambi-polar diffusion in which every electron particle was tied directly to the ion it was born with. These pairs of charged particles then move throughout the flow domain based on the velocity components of the ion particle. This method is reasonably successful, but it is difficult to implement and has poor performance at

high ionization levels. Carlson and Hassan [45] introduced a scheme in which electric fields are evaluated based on averaged charged particle properties. The charged particles are moved in these fields with the electrons processed at a significantly smaller time step than the ions. An alternate approach was proposed by Boyd [46] in which electron particles are moved throughout the domain based on cell-averaged ion velocities. The electron and ion particles are no longer tied together explicitly making the method much easier to implement and the approach is found to be generally more robust than Bird's technique. Using either of the Bird [44] or Boyd [46] approaches means that electron particles are moved at the time scale of the heavier species and so there is no need to reduce the simulation time step.

The second issue faced in simulating electrons, related to their significantly higher collision frequency, must also be addressed. The obvious choices are to either: (1) reduce the global time step; (2) allow electron particles to collide more than once over each iteration; or (3) perform sub-cycling of collisions. Sub-cycling involves calling the collision subroutine several times over each movement iteration so that the number of collision pairs to be tested is evaluated several times using a sub-cycling time step Δt_c that is smaller than the global time step Δt .

3.6 Radiation

Radiation is of interest in hypersonic flows in terms of the emission signature and at very high entry speeds for the radiative component of vehicle heating. Emission signatures are usually simulated decoupled from the flow field, and examples are discussed of such analysis in the second part of this article [8]. There have been several DSMC studies on emission signatures where the excited states of interest were simulated directly as additional chemical species [47,48]. A key issue here is the availability, or lack of it, of accurate excitation rate coefficients. For estimation of radiative heating, Bird first included thermal radiation effects in DSMC for analysis of an aero-assist orbital transfer vehicle [49,43] and his ideas were extended by Carlson and Hassan [50]. These models essentially represent an extension of the rotational and vibrational relaxation models using Borgnakke-Larsen energy disposal. As a phenomenological approach, these models performed reasonably well, but this is an area where further research is warranted.

3.7 Gas-Surface Interaction

The most important outcome from most DSMC analyses of hypersonic entry flows is the determination of the properties at the vehicle surface and in particular the aerodynamic forces and moments, and the convective heat transfer. The surface properties are of course very sensitive to the model assumed in DSMC for gas-surface interaction. The most common gas-surface interaction model used in DSMC is fully *diffuse* reflection in which a particle reflects from the surface with new velocity components that are sampled from Maxwellian distributions characterized by the wall temperature (note that the velocity component normal to the surface is sampled from a biased Maxwellian distribution). In the diffuse model, the particle's internal energies are also sampled from the appropriate equilibrium distribution, such as Eq. (3.4) for rotation, using the wall temperature. The opposite limit to diffuse reflection is *specular* reflection in which the only change to the particle's properties is its velocity component normal to the surface that is simply reversed in sign. Many DSMC computations use an accommodation coefficient, α , to simulate a combination of diffuse and specular reflections such that $\alpha=1$ is fully diffuse, and $\alpha=0$ is fully specular. Real engineering surfaces generally require a value in the range of $\alpha=0.8-0.9$.

Figure 11 shows a comparison of measured [51] and computed distributions of argon atoms reflecting from a platinum surface. Clearly, the measured pattern is not reproduced by either of the specular or diffuse reflection models (and indeed cannot be reproduced by any combination of the two models). This type of comparison

led to the development of more sophisticated gas-surface interaction models for DSMC, for example the Cercignani-Lampis-Lord (CLL) model [52]. Such models tend to have a stronger theoretical basis, like using a reciprocity relation, and offer more control through use of additional parameters. Figure 12a shows DSMC computed particle reflection distributions for Mach 10 flow of N_2 over a flat plate [53] for a variety of different gas-surface interaction models. Fully diffuse reflection gives the cosine distribution. Fully specular reflection gives a distribution that is almost tangent to the surface. Through variation of the accommodation coefficients a_M and σ_T (the parameters in the CLL model), a wide range of reflected distributions can be generated that lie between the ideal limits of diffuse and specular reflection. Figure 12b compares profiles of the velocity component parallel to the flat plate measured by Cecil and McDaniel [54] using Planar Laser Induced Fluorescence (PLIF) and a number of DSMC computations using diffuse reflection and the CLL model with a range of model parameters. Note, at the surface, that both measurements and computations show a significant level of velocity slip. Such comparisons allow identification of appropriate parameter values for use in the CLL model. However, the use of such models is relatively limited due to the lack of this type of basic information to identify parameter values for real systems of interest. This is perhaps another area where computational chemistry can provide data bases that can be used to build more advanced DSMC physical models.

There are two important phenomena arising from gas-surface interaction under high Knudsen number conditions: *velocity slip* and *temperature jump*. The relatively low number of collisions experienced by a gas at high Kn means that the average velocity at the wall has a finite value, even for a surface with fully diffuse reflection. This phenomenon reduces shear stress and may affect separation. Similarly, due to the low collision rate, the temperature of the gas at the wall is not equilibrated with the surface. In a hypersonic flow where the wall temperature is cooler than the gas, this phenomenon leads to a reduction in heat transfer. These effects are naturally included in a DSMC simulation using the diffuse reflection and CLL models whereas the usual approach for CFD is to assume no slip and no temperature jump at a wall. The omission of these high Knudsen number surface phenomena in CFD partially explains some of the differences noted in the detailed comparisons under hypersonic flow conditions of DSMC and CFD reported in [6,7]. One approach to try and extend the usefulness of CFD into the high Knudsen number range is to employ velocity slip and temperature jump models, see for example [7]. However, while some of these models do improve the agreement between CFD and DSMC results for surface quantities, it is not always achieved with a corresponding improvement in the comparisons of the flow properties. This situation again illustrates the need to perform non-continuum computations of high Knudsen number flows using kinetic methods such as the DSMC technique.

4.0 SUMMARY

The direct simulation Monte Carlo method (DSMC) has evolved over more than 40 years into a powerful analysis tool for computation of kinetic nonequilibrium hypersonic entry flows. The heart of the technique is its detailed treatment of collisional phenomena including momentum exchange, relaxation of internal energy modes, chemistry, radiation, and gas-surface interaction. In this article, the current status of DSMC models for simulating these physical phenomena has been reviewed. It is demonstrated that the DSMC technique is able to simulate accurately strong nonequilibrium phenomena generated inside strong shock waves of noble gases. Detailed validation of rotational energy relaxation models is also demonstrated at the level of rotational energy distribution functions measured inside a strong shock wave. However, detailed measurements of such phenomena at the high temperature conditions of hypersonic entry flows are still missing. Both phenomenological and detailed, quantum transition DSMC models for vibrational relaxation were discussed. There are presently no measurements of vibrational energy distributions in hypersonic flows that allow evaluation of such models. Several different DSMC chemistry models are described and two of them

evaluated using detailed information obtained from *ab initio* computational chemistry analysis. In the absence of detailed measurements of reaction cross sections, such analyses appear very promising to help in the construction and evaluation of detailed DSMC thermochemistry models. Descriptions were also provided of the present status for DSMC computation of charged species (ions, electrons), and radiation. These are areas where further work is required. Finally, the status for DSMC computation of gas-surface interaction was reviewed. It is shown that the idealized models of diffuse and specular reflection are not able to accurately reproduce reflections measured under hypersonic conditions. While more sophisticated gas-surface interaction models have been developed, their use is limited due to the difficulty in determining constants in the models. Again, this appears to be an area where *ab initio* computational analysis may be useful for building improved DSMC modeling capabilities.

5.0 ACKNOWLEDGMENTS

The author gratefully acknowledges financial support from NASA through grants NCC3-989, NNX08AD02A, and NNX08AH37A.

6.0 REFERENCES

- [1] Vincenti, W.G. and Kruger, C.H., *Introduction to Physical Gas Dynamics*, Wiley, New York, 1965.
- [2] Bird, G.A., "Approach to Translational Equilibrium in a Rigid Sphere Gas," *Physics of Fluids*, Vol. 6, 1963, pp. 1518-1519.
- [3] Bird, G.A., *Molecular Gas Dynamics*, Oxford University Press, Oxford, 1976.
- [4] Bird, G.A., *Molecular Gas Dynamics and the Direct Simulation of Gas Flows*, Oxford University Press, Oxford, 1994.
- [5] Boyd, I.D., "Computation of Atmospheric Entry Flow About a Leonid Meteoroid," *Earth, Moon, and Planets*, Vol. 82, 2000, pp. 93-108.
- [6] Lofthouse, A.J., Boyd, I.D. and Wright, M.J., "Effects of Continuum Breakdown on Hypersonic Aerothermodynamics," *Physics of Fluids*, Vol. 19, 2007, Article 027105.
- [7] Lofthouse, A.J., Scalabrin, L.C., and Boyd, I.D., "Velocity Slip and Temperature Jump in Hypersonic Aerothermodynamics," *Journal of Thermophysics and Heat Transfer*, Vol. 22, 2008, pp. 38-49.
- [8] Boyd, I.D., "Direct Simulation Monte Carlo for Atmospheric Entry. 2: Code Development and Application Results," notes for VKI Shortcourse, *Nonequilibrium Gas Dynamics: From Physical Models to Hypersonic Flights*, September 2008.
- [9] Alder, B.J. and Wainwright, T.E., "Studies in Molecular Dynamics," *Journal of Chemical Physics*, Vol. 27, 1957, pp. 1208-1209.
- [10] Boyd, I.D., "Vectorization of a Monte Carlo Simulation Scheme for Nonequilibrium Gas Dynamics," *Journal of Computational Physics*, Vol. 96, 1991, pp. 411-427.

- [11] Dietrich, S. and Boyd, I.D., "Scalar and Parallel Optimized Implementation of the Direct Simulation Monte Carlo Method," *Journal of Computational Physics*, Vol. 126, 1996, pp. 328-342.
- [12] LeBeau, G. J., "A Parallel Implementation of the Direct Simulation Monte Carlo Method," *Computer Methods in Applied Mechanics and Engineering*, Vol. 174, 1999, pp. 319-337.
- [13] Bird, G.A., "Sophisticated Versus Simple DSMC," Proceedings of the 25th International Symposium on Rarefied Gas Dynamics, St. Petersburg, Russia, July 2006
- [14] Bird, G.A., "Monte Carlo Simulation in an Engineering Context," *Progress in Astronautics and Aeronautics*, Vol. 74, AIAA, New York, 1981, pp. 239-255.
- [15] Koura, K. and Matsumoto, H., "Variable Soft Sphere Molecular Model for Air Species," *Physics of Fluids A*, Vol. 4, 1992, pp. 1083-1085.
- [16] Alsmeyer, H., "Density Profiles in Argon and Nitrogen Shock Waves Measured by the Absorption of an Electron Beam," *Journal of Fluid Mechanics*, Vol. 74, 1976, pp. 497-513.
- [17] Pham-Van-Diep, G., Erwin, D., and Muntz, E.P., "Nonequilibrium Molecular Motion in a Hypersonic Shock Wave," *Science*, Vol. 245, 1989, pp. 624-626.
- [18] Farbar, E.D. and Boyd, I.D., "Simulation of FIRE II Reentry Flow Using the Direct Simulation Monte Carlo Method," AIAA Paper 2008-4103, June 2008.
- [19] Balakrishnan, J., Boyd, I.D., and Braun, D.G., "Monte Carlo Simulation of Vapor Transport in Physical Vapor Deposition of Titanium," *Journal of Vacuum Science & Technology A*, Vol. 18, 2000, pp. 907-916.
- [20] Boyd, I.D., "Analysis of Rotational Nonequilibrium in Standing Shock Waves of Nitrogen," *AIAA Journal*, Vol. 28, 1990, pp. 1997-1999.
- [21] Parker, J.G., "Rotational and Vibrational Relaxation in Diatomic Gases," *Physics of Fluids*, Vol. 2, 1959, pp. 449-462.
- [22] Borgnakke, C. and Larsen, P.S., "Statistical Collision Model for Monte Carlo Simulation of Polyatomic Gas Mixture," *Journal of Computational Physics*, Vol. 18, 1975, pp. 405-420.
- [23] Lumpkin, F.E., Haas, B.L., and Boyd, I.D., "Resolution of Differences Between Collision Number Definitions in Particle and Continuum Simulations," *Physics of Fluids A*, Vol. 3, 1991, pp. 2282-2284.
- [24] Boyd, I.D., "Relaxation of Discrete Rotational Energy Distributions Using a Monte Carlo Method," *Physics of Fluids A*, Vol. 5, 1993, pp. 2278-2286.
- [25] Robben, R. and Talbot, L., "Experimental Study of the Rotational Distribution Function of Nitrogen in a Shock Wave," *Physics of Fluids*, Vol. 9, 1966, pp. 653-662.
- [26] Millikan, R.C. and White, D.R., "Systematics of Vibrational Relaxation," *Journal of Chemical Physics*, Vol. 39, 1963, pp. 3209-3213.

- [27] Park, C., *Nonequilibrium Hypersonic Aerothermodynamics*, Wiley, New York, 1990.
- [28] Boyd, I.D., "Analysis of Vibration-Dissociation-Recombination Processes Behind Strong Shock Waves of Nitrogen," *Physics of Fluids A*, Vol. 4 (1), 1992, pp. 178-185.
- [29] Bergemann, F. and Boyd, I.D., "New Discrete Vibrational Energy Method for the Direct Simulation Monte Carlo Method," *Rarefied Gas Dynamics*, Progress in Astronautics and Aeronautics, AIAA, Washington, Vol. 158, 1994, p. 174.
- [30] Vijayakumar, P., Sun, Q. and Boyd, I.D., "Detailed Models of Vibrational-Translational Energy Exchange for the Direct Simulation Monte Carlo Method," *Physics of Fluids*, Vol. 11, 1999, pp. 2117-2126.
- [31] Kerner, E.H., "Note on the Forced and Damped Oscillator in Quantum Mechanics," *Canadian Journal of Physics*, Vol. 36, 1958, pp. 371-374.
- [32] Sharma, S.P., "Rotational and Vibrational Temperature Measurements in a Shock Tube," *Proceedings of the 18th International Shock Tube Symposium*, Sendai, Japan, 1991, pp. 683-690.
- [33] Haas, B.L. and Boyd, I.D., "Models for Direct Monte Carlo Simulation of Coupled Vibration-Dissociation," *Physics of Fluids A*, Vol. 5, 1993, pp. 478-489.
- [34] Hornung, H.G., "Induction Time for Nitrogen Dissociation," *Journal of Chemical Physics*, Vol. 56, 1972, pp. 3172-3174.
- [35] Bose, D. and Candler, G.V., "Thermal rate Constants of the $N_2 + O \rightarrow NO + N$ Reaction Using Ab Initio 3A" and 3A' Potential Energy Surfaces," *Journal of Chemical Physics*, Vol. 104, 1996, pp. 2825-2834.
- [36] Boyd, I.D., Bose, D., and Candler, G.V., "Monte Carlo Modeling of Nitric Oxide Formation Based on Quasi-Classical Trajectory Calculations," *Physics of Fluids*, Vol. 9, 1997, pp. 1162-1170.
- [37] Boyd, I.D., "Modeling Backward Chemical Rate Processes in the Direct Simulation Monte Carlo Method," *Physics of Fluids*, Vol. 19, 2007, Article 126103.
- [38] Gallis, M.A. and Harvey, J.K., "Maximum Entropy Analysis of Chemical Reaction Energy Dependence," *Journal of Thermophysics and Heat Transfer*, Vol. 10, 1996, pp. 217-223.
- [39] Koura, K., "A Set of Model Cross Sections for the Monte Carlo Simulation of Rarefied Real Gases: Atom-Diatom Collisions," *Physics of Fluids*, Vol. 6, 1994, pp. 3473-3486.
- [40] Boyd, I.D., "A Threshold Line Dissociation Model for the Direct Simulation Monte Carlo Method," *Physics of Fluids*, Vol. 8, 1996, pp. 1293-1300.
- [41] Rebick, C. and Levine, R.D., "Collision Induced Dissociation: A Statistical Theory," *Journal of Chemical Physics*, Vol. 58, 1973, pp. 3942-3952.
- [42] Boyd, I.D., "Nonequilibrium Chemistry Modeling in Rarefied Hypersonic Flows," *Chemical Dynamics in Extreme Environments*, edited by R. A. Dressler, World Scientific Press, Singapore, 2001, pp. 81-137.

- [43] Wysong, I.J., Dressler, R.A., Chiu, Y.H., and Boyd, I.D., "Direct Simulation Monte Carlo Dissociation Model Evaluation: Comparison to Measured Cross Sections," *Journal of Thermophysics and Heat Transfer*, Vol. 16, 2002, pp. 83-93.
- [44] Bird, G.A., "Nonequilibrium Radiation During Re-entry at 10 km/s," AIAA Paper 87-1543, June 1987.
- [45] Carlson, A.B. and Hassan, H.A., "Direct Simulation of Re-entry Flows With Ionization," *Journal of Thermophysics and Heat Transfer*, Vol. 6, 1992, pp. 400-404.
- [46] Boyd, I.D., "Monte Carlo Simulation of Nonequilibrium Flow in Low Power Hydrogen Arcjets," *Physics of Fluids*. Vol. 9, 1997, pp. 3086-3095.
- [47] Gallis, M.A. and Harvey, J.K., "Atomic Species Radiation from Air Modeled Using the Direct Simulation Monte Carlo Method," *Journal of Thermophysics and Heat Transfer*, Vol. 9, 1995, pp. 456-463.
- [48] Kossi, K.K., Boyd, I.D., and Levin, D.A., "Direct Simulation of High Altitude Ultra-Violet Emission From the Hydroxyl Radical," *Journal of Thermophysics and Heat Transfer*, Vol. 12, 1998, pp. 223-229.
- [49] Bird, G.A., "Direct Simulation of Typical AOTV Entry Flows," AIAA Paper 86-1310, June 1986.
- [50] Carlson, A.B. and Hassan, H.A., "Radiation Modeling With Direct Simulation Monte Carlo," *Journal of Thermophysics and Heat Transfer*, Vol. 6, 1992, pp. 631-636.
- [51] Hinchey, J.J. and Foley, W.M., "Scattering of Molecular Beams by Metallic Surfaces," *Rarefied Gas Dynamics*, edited by J.H. de Leeuw, Academic Press, New York, 1966, Vol. 2, p. 505.
- [52] Lord, R.G., "Some Extensions to the Cercignani-Lampis Gas Scattering Kernel," *Physics of Fluids A*, Vol. 3, 1991, pp. 706-710.
- [53] Padilla, J.F., and Boyd, I.D., "Assessment of Gas-Surface Interaction Models in DSMC Analysis of Rarefied Hypersonic Flow," AIAA Paper 2007-3891, June 2007.
- [54] Cecil, D.E. and McDaniel, J.C., "Planar Velocity and Temperature Measurements in Rarefied Hypersonic Flow Using Iodine LIF," AIAA Paper 2005-4695, June 2005.

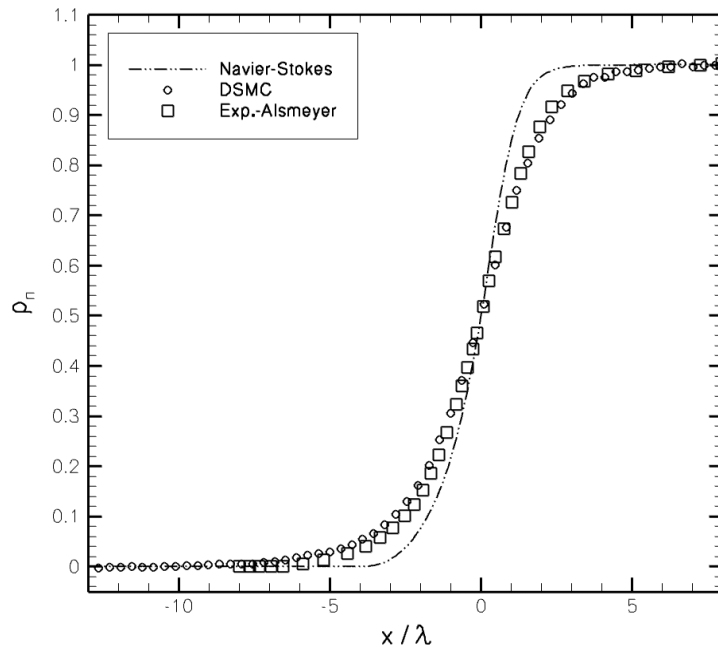


Figure 1a: Profiles of normalized density through a Mach 9 normal shock wave of argon: measurements from [16].

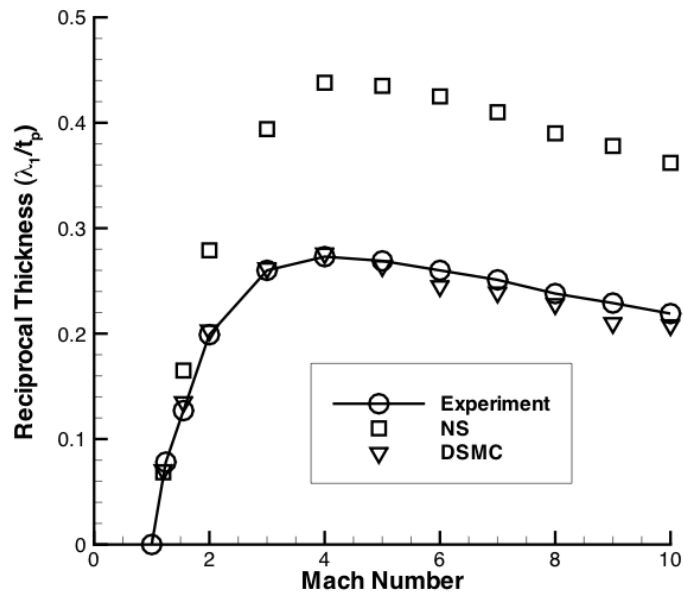


Figure 1b: Reciprocal shock thickness for normal shock waves of argon: measurements from [16].

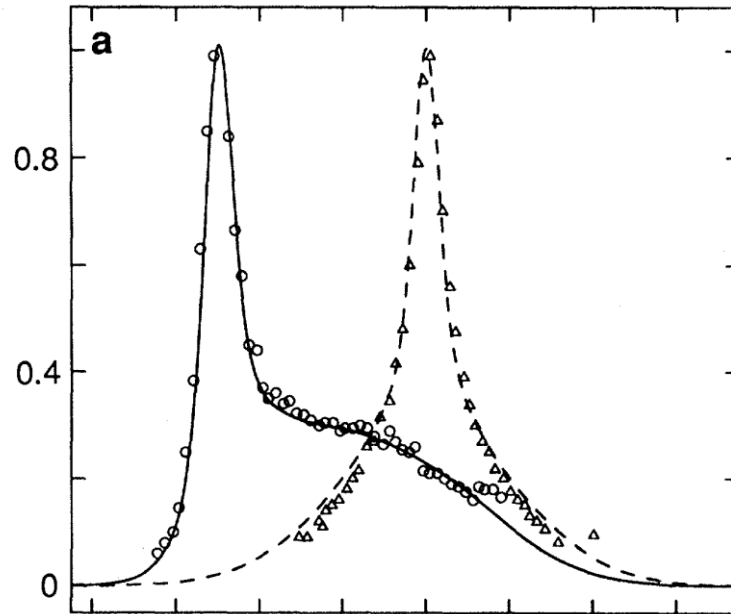


Figure 2a: Velocity distribution functions in the front a Mach 25 normal shock of helium: symbols = experiments; lines = DSMC [17].

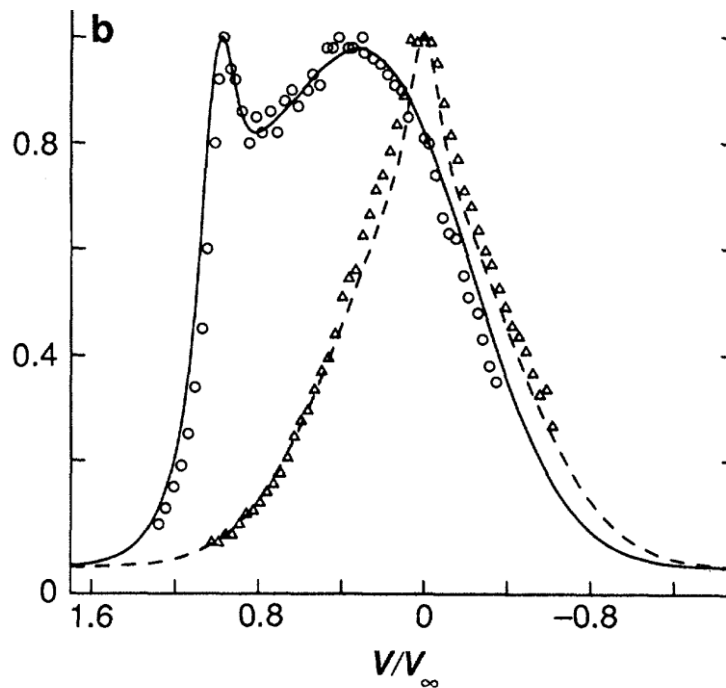


Figure 2b: Velocity distribution functions in the middle of a Mach 25 normal shock of helium: symbols = experiments; lines = DSMC [17].

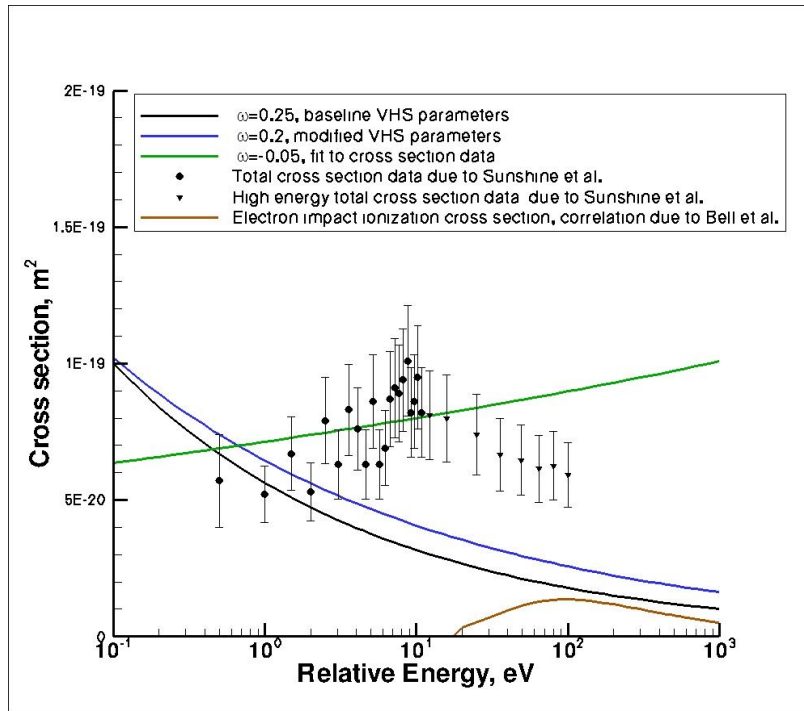


Figure 3a: Electron-oxygen atom collision cross sections [18].

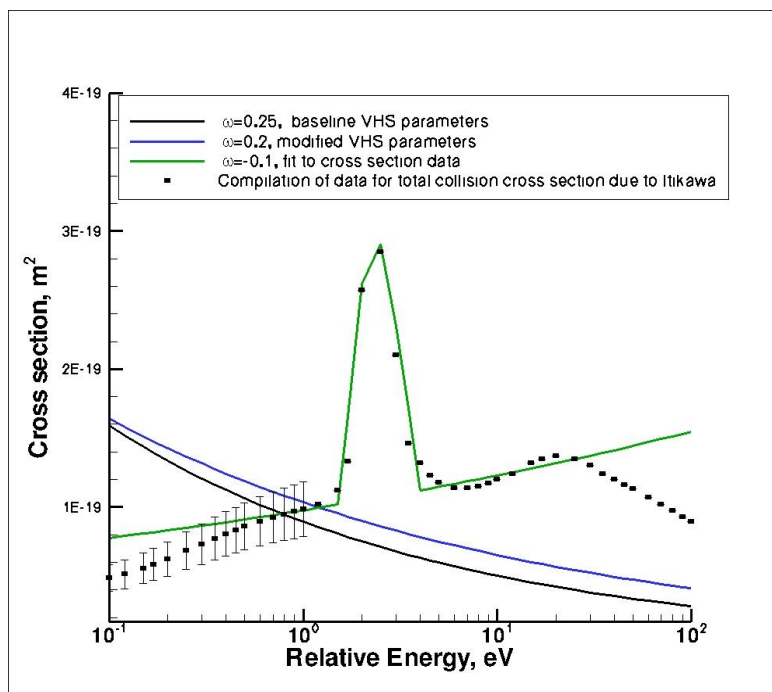


Figure 3b: Electron-nitrogen molecule collision cross sections [18].

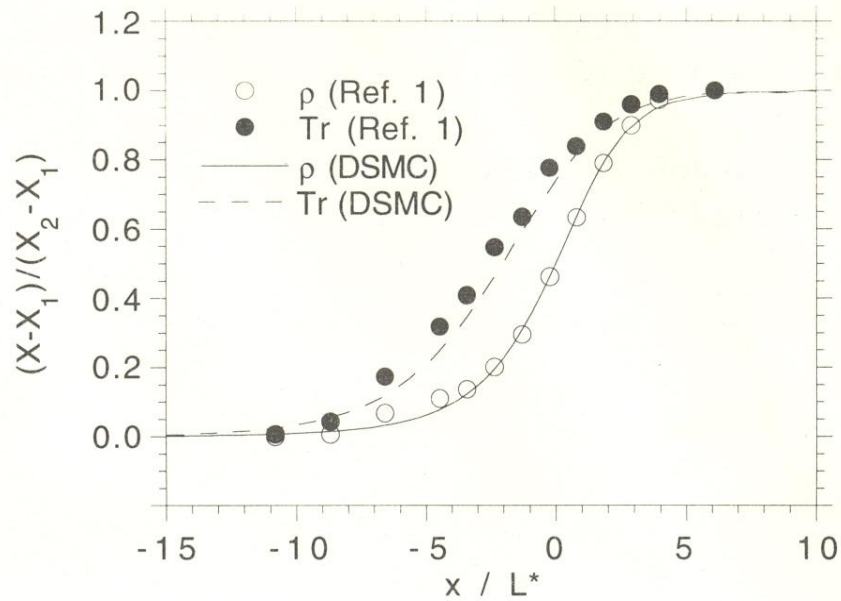


Figure 4a: Profiles of density and rotational temperature in a Mach 12.9 normal shock of N_2 [24].

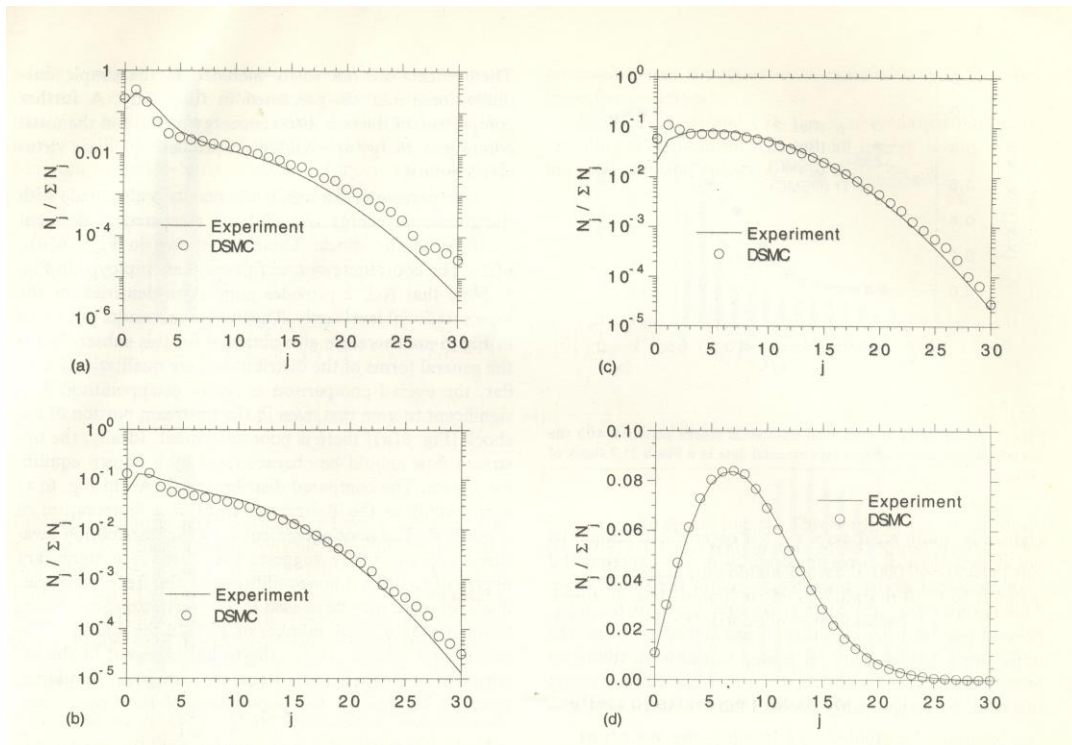


Figure 4b: Rotational energy distribution functions at four different locations in a Mach 12.9 normal shock of N_2

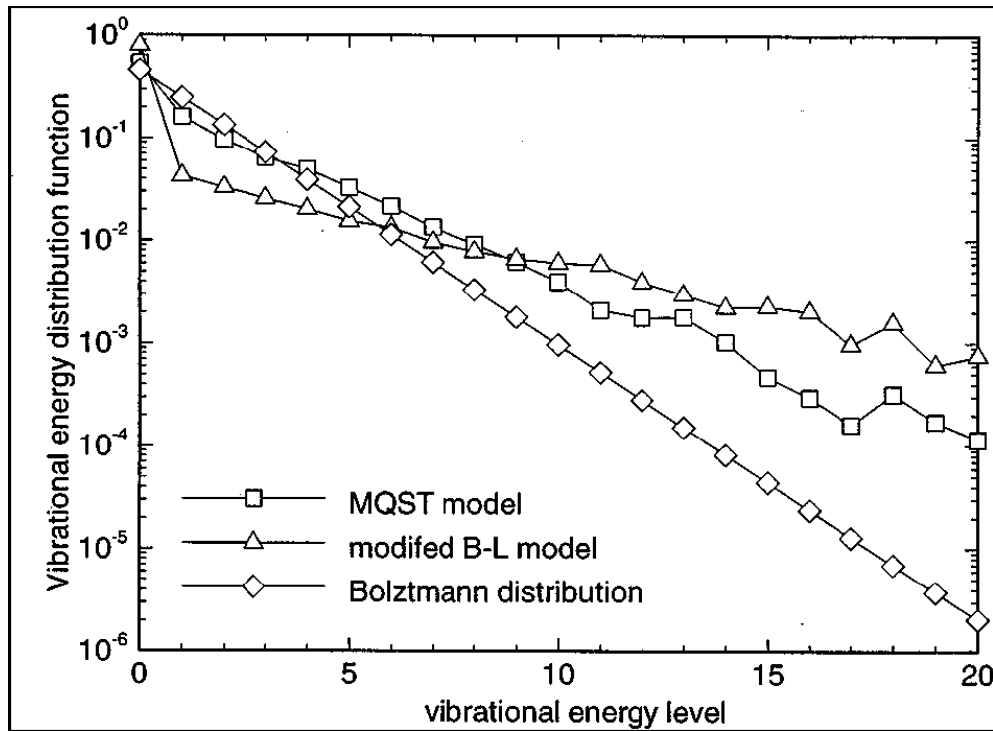


Figure 5: Vibrational energy distribution functions in the shock layer of N₂ flow over a sphere at 5.1 km/s and 80 km altitude [30].

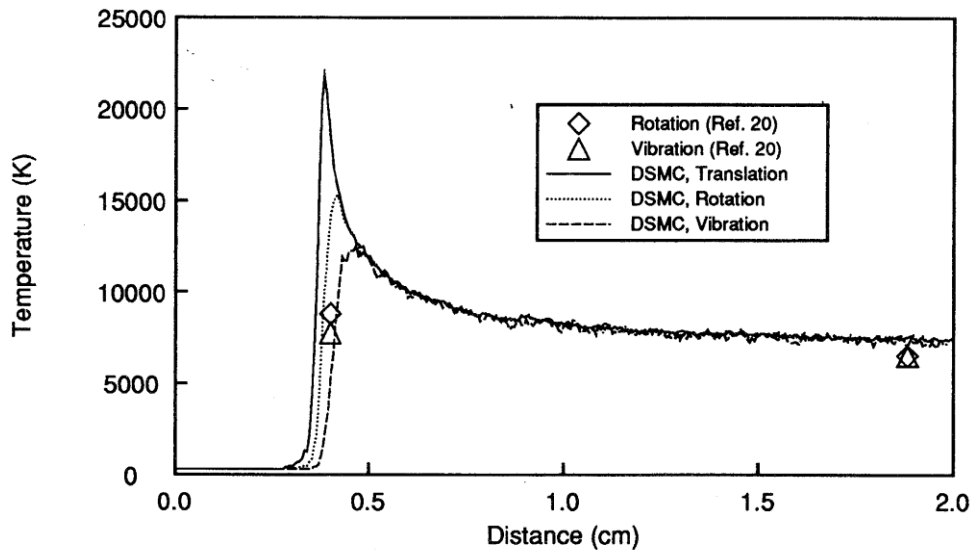


Figure 6: Temperature profiles in a Mach 17.8 normal shock wave of N₂ [28].

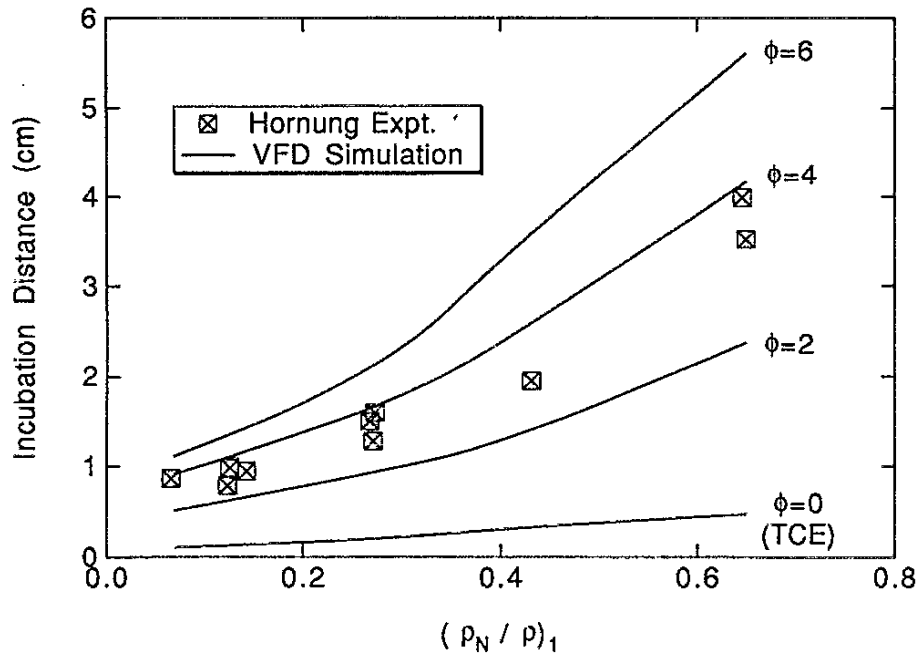


Figure 7: Dissociation incubation distance as a function of atom mass fraction [33].

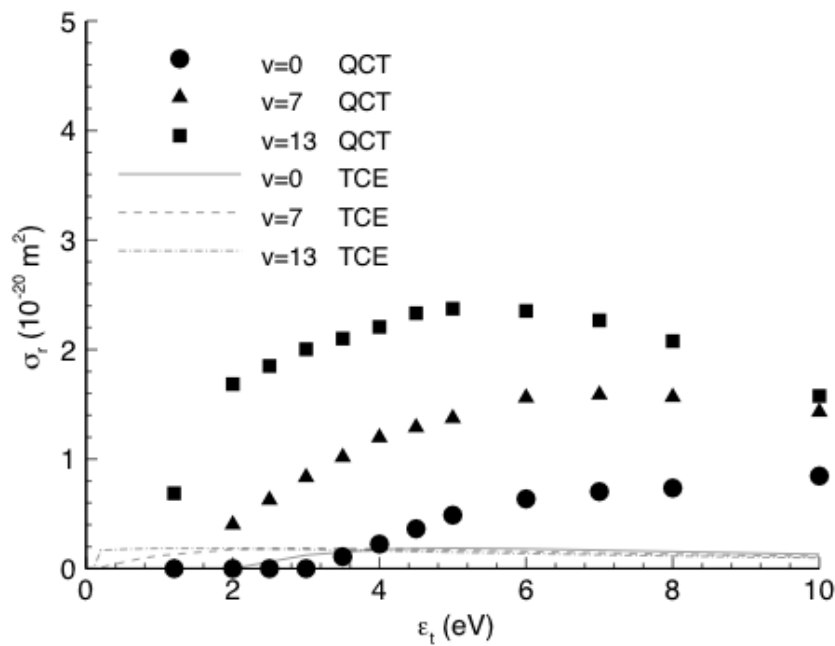


Figure 8a: Reaction cross sections at J=64 for nitric oxide formation [36].

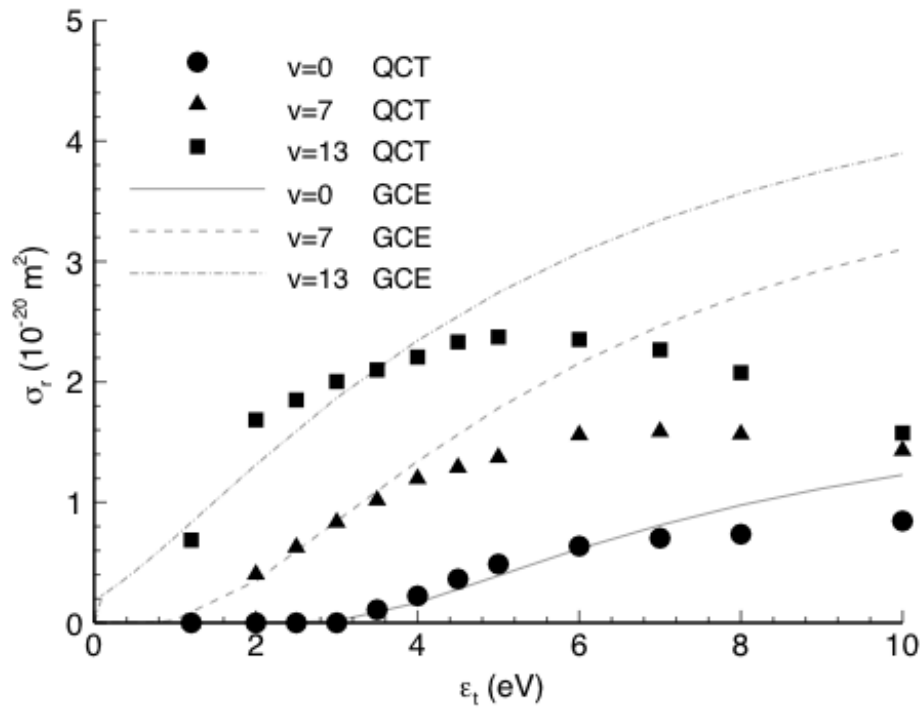


Figure 8b: Reaction cross sections at $J=64$ for nitric oxide formation [36].

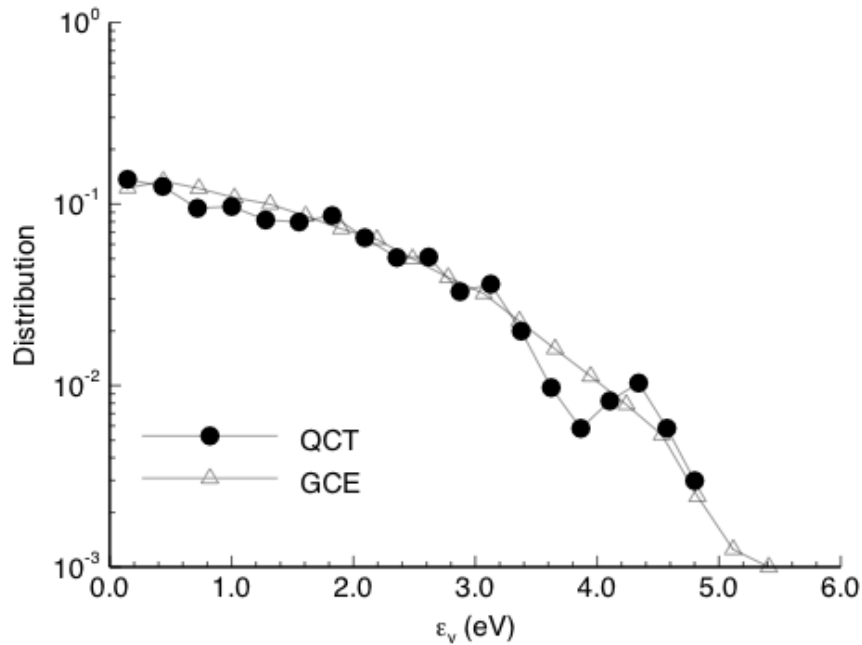


Figure 9a: Vibrational energy distribution function of reactants in nitric oxide formation: $T_t=T_r=T_v=5,000\text{K}$ [36].

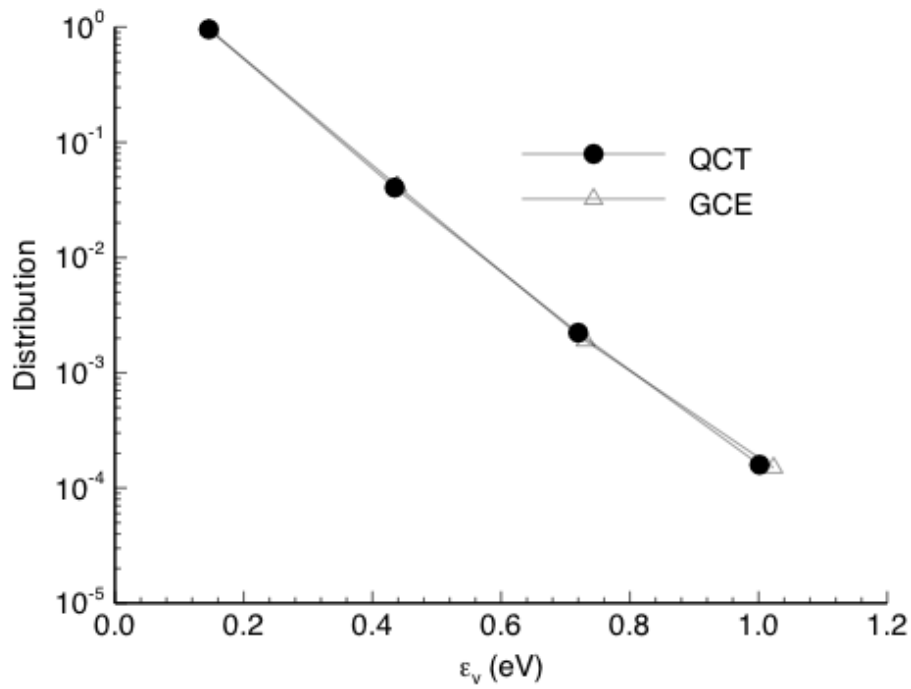


Figure 9b: Vibrational energy distribution function of reactants in nitric oxide formation: $T_t=14,000\text{K}$, $T_r=5,000\text{K}$, $T_v=1,000\text{K}$ [36].

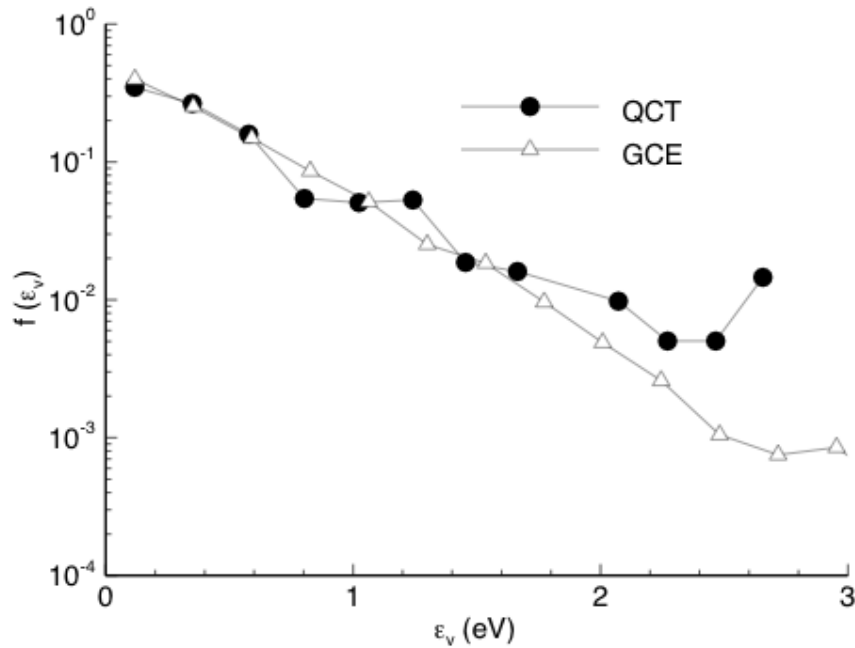


Figure 10a: Vibrational energy distribution function of products in nitric oxide formation: $T_t=T_r=T_v=5,000\text{K}$ [36].

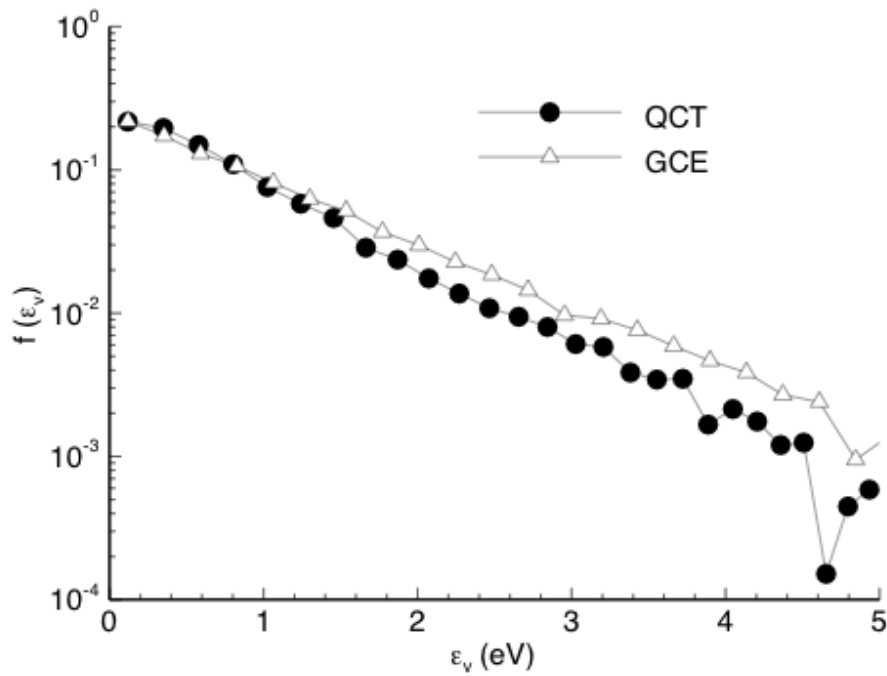


Figure 10b: Vibrational energy distribution function of products in nitric oxide formation: $T_t=14,000\text{K}$, $T_r=5,000\text{K}$, $T_v=1,000\text{K}$ [36].

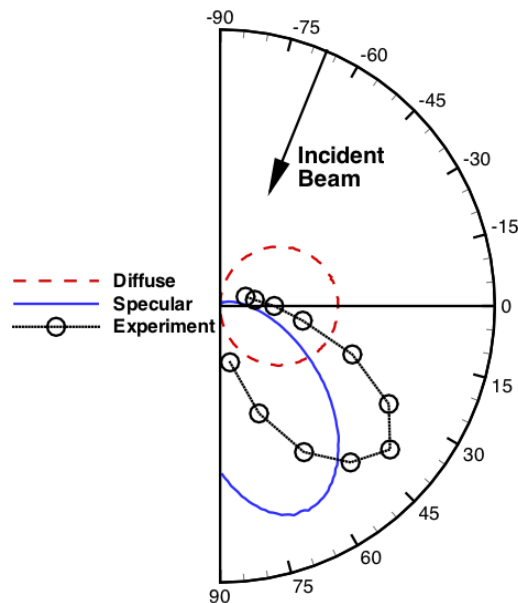


Figure 11: Distributions of Ar scattering from platinum: measurements from [51].

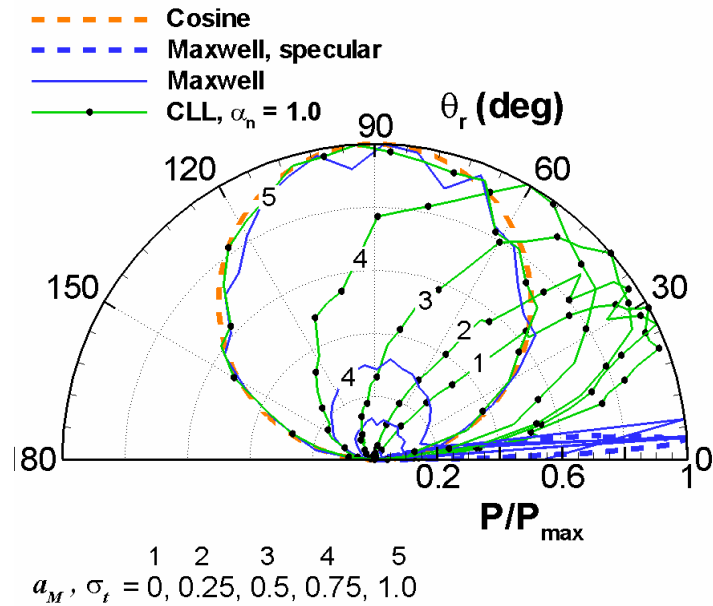


Figure 12a: DSMC computed scattering distributions from a DSMC simulation of hypersonic flow of N_2 over a flat plate [53].

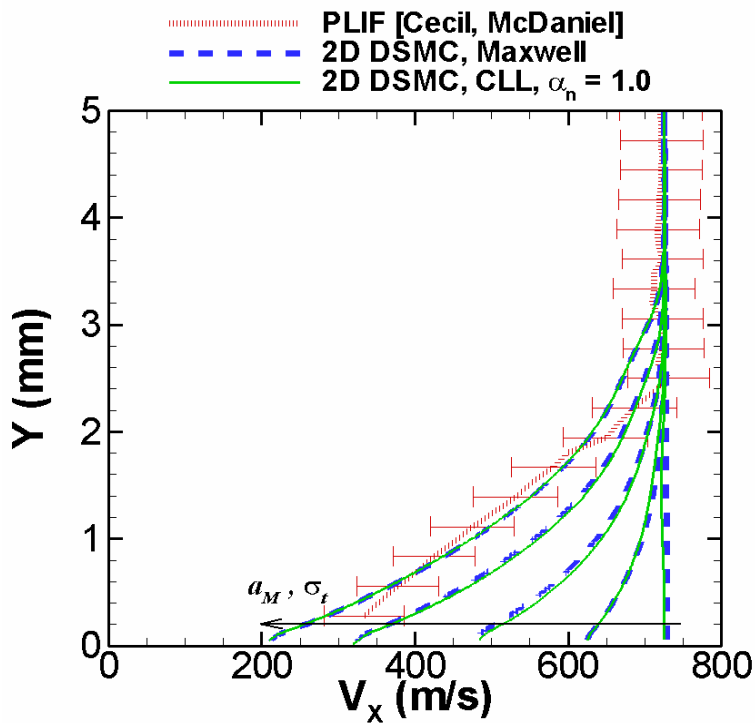


Figure 12b: Velocity profiles for hypersonic flow of N_2 over a flat plate [53].

